AIP | Applied Physics Letters

Electron spin resonance signature of the oxygen vacancy in HfO2

R. Gillen, J. Robertson, and S. J. Clark

Citation: Applied Physics Letters **101**, 102904 (2012); doi: 10.1063/1.4751110
View online: http://dx.doi.org/10.1063/1.4751110
View Table of Contents: http://scitation.aip.org/content/aip/journal/apl/101/10?ver=pdfcov
Published by the AIP Publishing

Electron spin resonance signature of the oxygen vacancy in HfO_2

R. Gillen,[1] J. Robertson,[1] and S. J. Clark[2]
[1]*Engineering Department, Cambridge University, Cambridge CB2 1PZ, United Kingdom*
[2]*Physics Department, Durham University, Durham, United Kingdom*

(Received 20 July 2012; accepted 23 August 2012; published online 6 September 2012)

The oxygen vacancy has been inferred to be the critical defect in HfO_2, responsible for charge trapping, gate threshold voltage instability, and Fermi level pinning for high work function gates, but it has never been conclusively identified. Here, the electron spin resonance g tensor parameters of the oxygen vacancy are calculated, using methods that do not over-estimate the delocalization of the defect wave function, to be $g_{xx} = 1.918$, $g_{yy} = 1.926$, $g_{zz} = 1.944$, and are consistent with an observed spectrum. The defect undergoes a symmetry lowering polaron distortion to be localized mainly on a single adjacent Hf ion. © *2012 American Institute of Physics*. [http://dx.doi.org/10.1063/1.4751110]

HfO_2 has now replaced SiO_2 as the gate dielectric in metal oxide semiconductor field effect transistors (MOSFET).[1] Further scaling of MOSFETs is likely to involve the continued use of HfO_2 plus thinning of the interfacial SiO_2 layer[2] rather than by using higher dielectric constant (K) oxides. Any degradation of the HfO_2 dielectric such as charge trapping,[3,4] bias stress instability,[5,6] channel mobility reduction,[7] or band bending in the oxide next to a high work function gate electrode[8–11] has generally been attributed to oxygen vacancies. Similarly, non-volatile memories are now taking an increasing importance in modern portable electronics, where the non-volatile resistive random access memory (RRAM) is a leading candidate to superceded Flash memory technology. RRAM devices, consisting of a high K oxide between two electrodes, operate by the formation of a conductive filament across the oxide. This filament is generally believed to be a path of oxygen vacancies.[12–15] Nevertheless, in both types of device, the attribution to oxygen vacancies is based on electrical data, optical spectra, and internal consistency.[4,6,11,13,15–18] There has been no fully accepted chemical identification of the oxygen vacancy in HfO_2 by, say, electron spin resonance (ESR).[19–21] This situation differs from the oxygen vacancy in TiO_2[22] and contrasts strongly with the vast literature on the paramagnetic E′ and P_b centers in SiO_2.[23,24] In this paper, we explain the problems with the symmetry assignment of the oxygen vacancy in HfO_2 in previous calculations and present a calculation of the ESR signature of the O vacancy using hybrid density functional methods, to help aid this identification.

We first note the previous work on the attribution of degradation effects in HfO_2 to the O vacancy. Cartier *et al.*[4] found a strong correlation between the defect density seen by charge pumping and the bias stress data. Guha[11] argued that the defect thermodynamics are consistent with assigning the defect to an O vacancy based on a comparison with similar oxides like $SrTiO_3$. The observed energy levels of the defect from charge trapping,[3] charge pumping spectra,[4] optical absorption,[16] and cathodo-luminescence spectra[17] are all consistent with the calculated energy levels.[18] In ESR, Kang *et al.*[19] have observed various paramagnetic defects such as the peroxyl radical in atomic layer deposited (ALD) HfO_2. Wright and Barklie[20] observed a number of low symmetry defects in HfO_2 powders and thin films that they associated with under-coordinated Hf^{3+} sites. Stesmans[21] observed the P_b center in HfO_2 on Si, but this was associated with the SiO_2 interlayer not the HfO_2 itself. Meanwhile, there were previous reports on paramagnetic defects in ZrO_2 and Y-stabilized ZrO_2 that were associated with Zr^{3+} sites,[25–27] but these were in bulk or nanocrystalline material not of electronic grade.

The most notable feature is that the observed signatures of Hf^{3+} or Zr^{3+} defects do not correspond to those predicted by electronic structure calculations. The observed ESR signal usually has axial symmetry, with the charge localized on a single adjacent Hf ion, whereas electronic structure calculations of the positively charged oxygen vacancy, V^+, generally find that the unpaired spin is usually delocalized across all adjacent Hf neighbors of the defect.[28–33] This led to speculation that the defect could be a vacancy localized at a grain boundary or interface, or be a divacancy.[34]

It turns out that this symmetry problem is a standard error of density functional theory (DFT).[35,36] DFT represents the many-particle exchange-correlation energy as a function of the electron density. However, DFT has the well-known error that it under-estimates the semiconductor band gaps, and a less well-known error of giving defect wavefunctions that are too delocalized. Both effects are due to a lack of self-interaction correction. A good example is that DFT finds that the hole trapped at a substitutional Al_{Si} site in quartz ("smoky" quartz) is localized over all four oxygen neighbors, whereas ESR shows that the hole is localized on just one oxygen neighbor.[35] Another example is that the hole localizes on only one of the four O neighbors at the Zn vacancy in ZnO.[37]

A simple solution to this problem is to use hybrid functionals such as Heyd, Scuseria, Ernzerhof (HSE),[38] screened exchange (sX),[39] or PBE0 functionals. These functionals mix a fraction of Hartree-Fock exchange into the DFT exchange-correlation energy. This corrects the band gap and the localization errors. Hybrid functionals have the advantage that they are generalized Kohn-Sham functionals in the DFT sense, so that they can be used variationally for energy minimization to calculate atomic geometries. This is critical, because wavefunction localization is tied to the atomic geometry as in a polaron,[36] so that if the geometry is wrong, the wavefunction is also wrong.

We previously calculated the electronic structure of V^+ by sX using the CASTEP plane wave code. This used 96

atom supercells of monoclinic HfO_2. The supercell structure is relaxed at constant volume for each charge state. Charge state and finite cell corrections are included as in Lany.[40] The wavefunction of the V^+ shows the correct localization on mainly a single adjacent Hf ion.[41] However, CASTEP does not presently give ESR parameters. Therefore, the calculation was repeated for HfO_2 clusters including a vacancy using the ORCA local orbital code,[42] which does provide ESR parameters. ORCA does not yet include screened exchange. We thus choose to use the BH and HLYP hybrid functional,[43] as this yields geometries and charge densities that are in good agreement with those of sX.

We used the defect geometries from the sX supercells embedded them in a supercell of ideal monoclinic HfO_2 and cut out two clusters containing 81 atoms for the 3-fold vacancy and 95 atoms for the 4-fold vacancy surrounding the defect. The oxygen atoms at the cluster surface were then passivated by hydrogen atoms to restore charge neutrality to the cluster. The hydrogen atoms were described by an all-electron double-zeta + polarization (DZP) basis set,[44] while we employed a combination of split-valence triple-zeta (TZV) basis sets,[45] which are tailored to the Douglas-Kroll-Hess scalar-relativistic Hamiltonian, and the polarization functions from def2-split-valence triple-zeta + polarization (TZVP) basis sets for the hafnium and oxygen atoms.

The formation energy of the defects from the supercell calculations is plotted in Fig. 1 as a function of the Fermi energy for the 3-fold O vacancy (the 3-fold vacancy is slightly more stable than the 4-fold vacancy.) We see that the O vacancy has 5 possible charge states, two positive and two negative. The neutral and positive states are expected due to the electronegative character of missing O^{2-} ion. The V^- state is very important and is the trapping level.[18] On the other hand, the V^+ and V^{2+} charge states are critical for the band-bending problem.[10]

For the neutral vacancy, the adjacent Hf ions do not relax much compared to their ideal positions. For V^+ and V^{2+}, the adjacent Hf ions relax away from the vacancy site. Previously, for V^+ in DFT, this relaxation was symmetric. In that case, the unpaired electron of V^+ is equally spread over the 3 or 4 nearest neighbors, as seen in the charge density in Fig. 2.

In contrast, in sX, two of the three Hf ions of V^+ relax further away from the vacancy site in a polaron distortion.

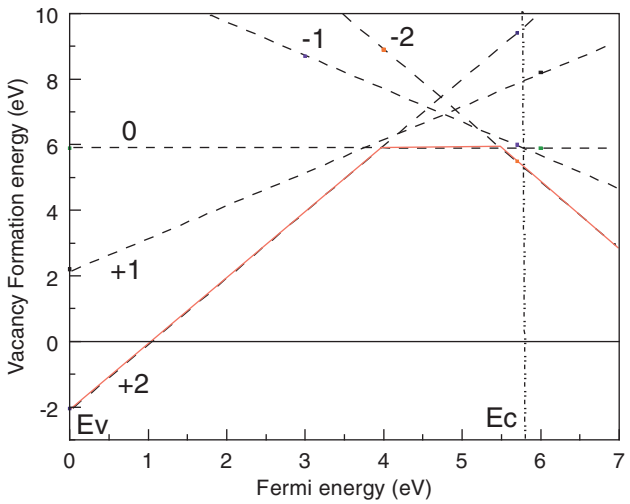

FIG. 1. Formation energy of the O vacancy vs. Fermi in HfO_2 for $\mu_O = 0$ eV (O rich limit) in sX. The slopes of the lines are the charge states, and the crossing points are the transition energies. Those around 4 eV are for 0/+ and 0/2+, those around 5.5 eV are 0/−.

This localizes the electron mainly onto a single Hf site, as seen in the charge density map in Figs. 3(a) and 3(b). This gives a defect of near axial symmetry. This asymmetric relaxation will only occur for the hybrid functionals or Hartree-Fock itself; simple DFT always converges to the symmetric case.

The principal values of the corresponding ESR g-tensor from ORCA are given in Table I. The V_O^+ causes a single occupied defect level in the upper band gap. As expected for an "electron-like" state, the calculated g-tensor values are noticeably below the g-factor of a free electron, $g_e = 2.0023$. The polaronic distortion of the geometry around the defect shows in the asymmetry of the principal value of the g-tensor. Our g-tensors of both oxygen vacancies have orthorhombic symmetry, with $g_1 = 1.918$, $g_2 = 1.926$, $g_3 = 1.944$ for the three-fold vacancy (V_{O3}^+), and $g_1 = 1.929$, $g_2 = 1.947$, $g_3 = 1.967$ for the four-fold vacancy (V_{O4}^+). These values are fairly similar to the g-tensors reported by Munoz Ramo *et al.*[33] in their B3LYP calculation.

There are three existing ESR experiments on HfO_2. For ALD HfO_2 on Si, Kang and Lenahan[22] detected two defects, one a clear signature of the peroxyl radical. Also for ALD HfO_2 on Si, Stesmans[24] detected the P_b defect, a Si dangling

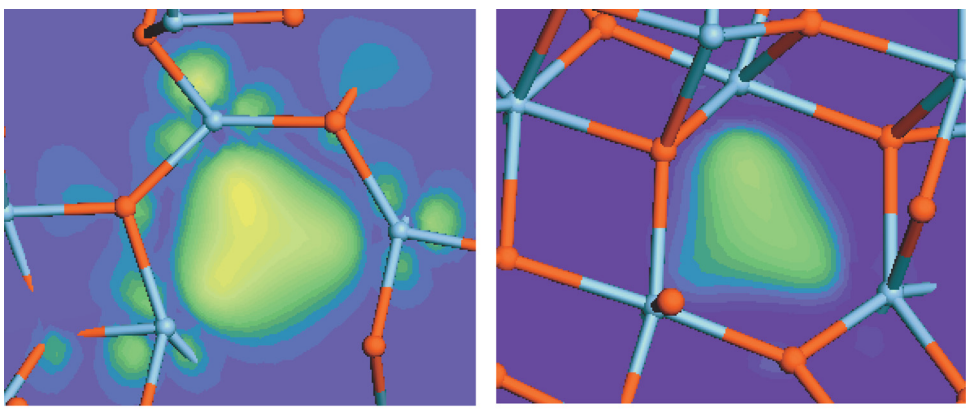

(a) (b)

FIG. 2. Symmetric A_1 orbital of the (a) three-fold coordinated and (b) four-fold coordinated O vacancies in HfO_2 as predicted by GGA calculations. In both cases, the defect state is delocalized of all Hf neighbors (blue balls). Oxygens are red balls.

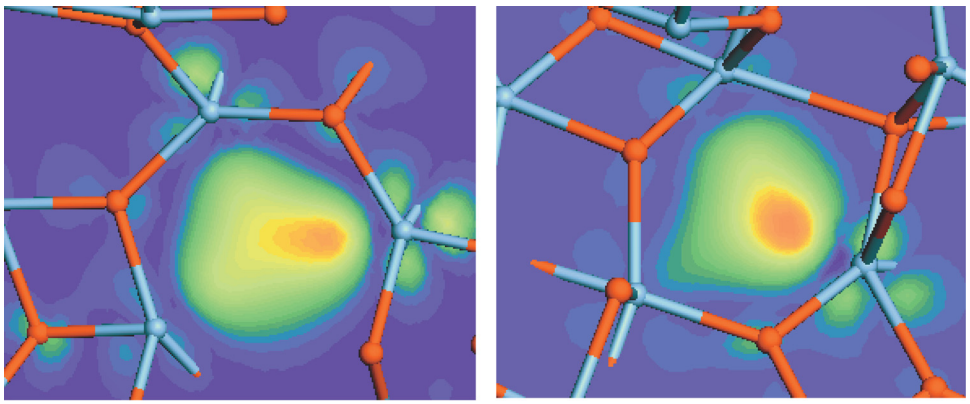

(a) (b)

FIG. 3. Calculated defect orbital of the (a) three-fold coordinated and (b) four-fold coordinated O vacancies in HfO_2 as predicted by BHandHLYP. The electron in the defect state is mainly localized one of the Hf ions adjacent to the vacancy.

TABLE I. Calculated and experimental components of the g-tensor for the single positively charged three-fold (O_{V3}^+) and four-fold (O_{V4}^+) oxygen vacancy.

Defect	g-tensor	This work	B3LYP[33]	Exp.[23]
V_{O3}^+	g_1	1.918	1.927	$g_{\parallel} = 1.938–1.941$
	g_2	1.926	1.938	
	g_3	1.944	1.960	$g_{\perp} = 1.970$
	g_{iso}			
V_{O4}^+	g_1	1.9296	1.945	
	g_2	1.947	1.963	
	g_3	1.967	1.9835	
	g_{iso}	1.9482		

bond on the Si side of the Si:HfO_2 interface, but could find no direct HfO_2 signature. Barklie and Wright[23] measured ESR for powder samples of HfO_2 and found a number of lower symmetry defects. They attributed a defect of axial symmetry to the oxygen vacancy or a related impurity. The g-tensor components of $g_{\parallel} = 1.938–1.941$ and $g_{\perp} = 1.970$ now fit well to our predictions for the oxygen vacancy and those of Munos-Ramo *et al.*,[33] but the axial symmetry is inconsistent with our findings. We can track the origin of the lacking axial symmetry to the defect wavefunction. While most of the orbital is localized at one of the Hf atoms, tails of lower density extend to the other Hf atoms around the vacancy. Clearly, not all of these Hf atoms contribute equally to the defect state, particularly in the case of V_{O4}^+, thus causing the orthorhombic symmetry of the g-tensor. On the other hand, the g-tensor for V_{O3}^+ almost axial-symmetric, g_1 and g_2 are quite similar, while g_3 is considerably larger.

Our work also resolves the identification of defects in the chemical similar ZrO_2 where ESR usually finds the state localized on a single Zr^{3+} ion.[25,26] Similarly, for oxygen vacancies on the surface of TiO_2, the defect wavefunction becomes localized on a single Ti^{3+} ion,[22] and also in theory, when the correct calculation method is used.[46] Our work could allow the role of oxygen vacancies in the switching mechanism in HfO_2 RRAM to be studied, by using the much more sensitive electrically detected magnetic resonance method.[47]

In summary, we have shown how a symmetry-lowering distortion at the O vacancy in HfO_2 leads to ESR g tensors now in agreement with experiment. Interestingly, this replicates the history of the E′ O vacancy center in SiO_2, in which a symmetry-lowering distortion[48] was only identified 18 years after its discovery.[49]

[1]J. Robertson, Rep. Prog. Phys. **69**, 327 (2006).
[2]T. Ando, M. M. Frank, K. Choi, C. Choi, J. Bruley, M. Hopstaken, M. Copel, E. Cartier, A. Kerber, A. Callegari *et al.*, Tech. Dig. - Int. Electron Devices Meet. (2009); L. A. Ragnarsson, T. Chiarella, M. Togo, T. Schram, P. Absil, and T. Hoffmann, Microelectron. Eng. **88**, 1317 (2011).
[3]A. Kerber, E. Cartier, L. Pantisano, R. Degraeve, T. Kauerauf, Y. Kim, G. Groesenken, H. E. Maes, and U. Schwalke, IEEE Electron Device Lett. **24**, 87 (2003).
[4]E. Cartier, B. Linder, V. Narayanan, and V. Paruchuri, Tech. Dig. – Int. Electron Devices Meet. **2006**, 321.
[5]S. Zafar, S. Callegari, E. Gusev, and M. V. Fischetti, J. Appl. Phys. **93**, 9298 (2003).
[6]E. Cartier, A. Kerber, T. Ando, M. M. Frank, K. Choi, S. Krishnan, B. Linder, K. Zhao, F. Monsieur, J. Stathis, and V. Narayanan, Tech. Dig. – Int. Electron Devices Meet. **2011**, 18.4.
[7]S. Saito, D. Hisamoto, S. Kimura, and M. Hiratani, Tech. Dig. – Int. Electron Devices Meet. **2003**, 33.3.
[8]J. K. Schaeffer, L. R. C. Fonseca, S. B. Samavedam, P. J. Tobin, and B. E. White, Appl. Phys. Lett. **85**, 1826 (2004).
[9]E. Cartier, F. McFeely, V. Narayanan, M. Copel, S. Guha, R. Jammy, and G. Shahidi, Dig. Tech. Pap. – Symp. VLSI Technol. **2005**, 15.
[10]K. Shiraishi, K. Yamada, K. Torii, Y. Akasaka, K. Nakajima, M. Konno, T. Chikyow, H. Kitajima, and T. Arikado, Jpn. J. Appl. Phys., Part 2 **43**, L1413 (2004); Y. Akasaka, G. Nakamura, K. Shiraishi, N. Umezawa, K. Yamabe, O. Ogawa, M. Lee, T. Amiaka, T. Kasuya, H. Watanabe *et al.*, Jpn. J. Appl. Phys., Part 2 **45**, L1289 (2006); J. Robertson, O. Sharia, and A. Demkov, Appl. Phys. Lett. **91**, 132912 (2007).
[11]S. Guha and V. Narayanan, Phys. Rev. Lett. **98**, 196101 (2007); S. Guha and P. Solomon, Appl. Phys. Lett. **92**, 012909 (2008).
[12]R. Waser, R. Dittman, G. Staikov, and K. Szot, Adv. Mater. **21**, 2632 (2009).
[13]G. Bersuker, J. Appl. Phys. **110**, 124518 (2011).
[14]S. Clima, Y. Chen, M. Mees, K. Sankaran, B. Govoreanu, M. Jurczak, S. DeGendt, and G. Pourtois, Appl. Phys. Lett. **100**, 133102 (2012).
[15]S. G. Park, B. Magyari-Knope, and Y. Nishi, IEEE Electron Device Lett. **32**, 197 (2011).
[16]H. Takeuchi, D. Ha, and T. J. King, J. Vac. Sci. Technol. A **22**, 1337 (2004).
[17]S. Walsh, L. Fang, J. K. Schaeffer, E. Weisbrod, and L. J. Brillson, Appl. Phys. Lett. **90**, 052901 (2007).
[18]K. Xiong, J. Robertson, M. C. Gibson, and S. J. Clark, Appl. Phys. Lett. **87**, 183505 (2005).
[19]A. Y. Kang, P. M. Lenahan, and J. F. Conley, Appl. Phys. Lett. **83**, 3407 (2003).
[20]R. C. Barklie and S. Wright, J. Appl. Phys. **106**, 103917 (2009).
[21]A. Stesmans and V. V. Afanasev, Appl. Phys. Lett. **82**, 4074 (2003).
[22]S. Yang, L. E. Halliburton, A. Manivannan, P. H. Bunton, D. B. Baker, M. Klemm, S. Horn, and A. Fujishima, Appl. Phys. Lett. **94**, 162114 (2009).
[23]D. L. Griscom, J. Non–Cryst. Solids **73**, 51 (1985); Phys. Rev. B **20**, 1823 (1979).
[24]E. Poindexter, G. J. Gerardi, M. E. Ruckel, and P. J. Caplan, J. Appl. Phys. **56**, 2844 (1984).

[25]C. Morterra, E. Giamello, L. Orio, and M. Volante, J. Phys. Chem. **94**, 3111 (1990).
[26]J. Matta, J. F. Lamonier, E. Abi-Aad, Z. Zhilinskaya, and A. Aboukais, Phys. Chem. Chem. Phys. **1**, 4975 (1999).
[27]T. Morimoto, M. Takase, T. Ito, H. Kato, and Y. Ohki, Jpn. J. Appl. Phys., Part 1 **47**, 6858 (2008).
[28]A. S. Foster, F. L. Gejo, A. L. Shluger, and R. N. Nieminen, Phys. Rev. B **65**, 174117 (2002).
[29]Y. P. Feng, A. T. Lim, and M. F. Li, Appl. Phys. Lett. **87**, 062105 (2005).
[30]E. A. Choi and K. J. Chang, Appl. Phys. Lett. **94**, 122901 (2009).
[31]A. Broqvist and A. Pasquarello, Appl. Phys. Lett. **89**, 262904 (2007).
[32]J. L. Gavartin, D. M. Ramo, A. Shluger, G. Bersuker, and B. H. Lee, Appl. Phys. Lett. **89**, 082908 (2006).
[33]D. Munoz-Ramo, J. L. Gavartin, A. L. Shluger, and G. Bersuker, Phys. Rev. B **75**, 205336 (2007).
[34]G. Lucovsky, K. B. Chung, and J. W. Kim, Microelectron. Eng. **86**, 1676 (2006).
[35]G. Pacchioni, F. Frigoli, D. Ricci, and J. A. Weil, Phys. Rev. B **63**, 054102 (2000).
[36]S. Lany and A. Zunger, Phys. Rev. B **80**, 085202 (2009).
[37]S. J. Clark, J. Robertson, S. Lany, and A. Zunger, Phys. Rev. B **81**, 115311 (2010).
[38]J. Heyd, G. E. Scuseria, and M. Ernzerhof, J. Chem. Phys. **118**, 8207 (2003).
[39]S. J. Clark and J. Robertson, Phys. Rev. B **82**, 085208 (2010).
[40]S. Lany and A. Zunger, Phys. Rev. B **78**, 235104 (2008).
[41]S. J. Clark, L. Lin, and J. Robertson, Microelectron. Eng. **88**, 1464 (2011).
[42]F. Neese, J. Chem. Phys. **122**, 034107 (2005).
[43]A. D. Becke, J. Chem. Phys. **98**, 5648 (1993).
[44]The Ahlrichs DZP basis set is from the TurboMole basis set library of K. Eichkorn, F. Weigend, O. Treutler, and R. Ahlrichs, Theor. Chem. Acc. **97**, 119 (1997).
[45]D. A. Pantazis, X. Y. Chen, C. R. Landis, and F. Neese, J. Chem. Theory Comput. **4**, 908 (2008).
[46]C. DiValentin, G. Pacchioni, and A. Selloni, Phys. Rev. Lett. **97**, 166803 (2006).
[47]S. Baldovino, A. Molle, and M. Fanciulli, Appl. Phys. Lett. **93**, 242105 (2008).
[48]F. J. Feigl, W. B. Fowler, and K. L. Yip, Solid State Commun. **14**, 225 (1974).
[49]R. A. Weeks, J. Appl. Phys. **27**, 1376 (1956).